Computer-Aided Design of Millimeter-Wave *E*-Plane Filters

YI-CHI SHIH, STUDENT MEMBER, IEEE, TATSUO ITOH, FELLOW, IEEE, AND L. Q. BUI

Abstract—**A computer-aided design (CAD) algorithm has been developed for a class of *E*-plane bandpass filters. The analysis portion of the algorithm is based on the residue-calculus technique and a generalized scattering parameter method. It is mathematically exact and numerically very efficient. Filters designed with this method have been fabricated and tested in *Ka*-band. Good agreement with design has been obtained.**

I. Introduction

SEVERAL FILTER CIRCUITS that are composed of a conductive sheet which is properly designed and sandwiched between the waveguide shells parallel to the *E*-plane have been proposed recently [1]–[5]. The circuits are developed either on a metal sheet [1], [2] or on a bilateral fin-line [3]–[5]. In these filters, the slot widths are equal to the waveguide height; thereby the structure really consists of several resonators separated by printed inductive strips. Since the structures, especially those in forms of fin-lines, are amenable to photolithographic techniques and only straight line shapes are involved, they are highly suitable for mass production. Some design procedures have been reported based on a number of methods such as mode-matching techniques and variational techniques. These methods have been applied only to metallic *E*-plane circuits or bilateral fin-line structures.

This paper presents a new efficient computer-aided design (CAD) algorithm developed for a class of *E*-plane bandpass filters. A unified treatment is introduced which applies not only to the purely metallic *E*-plane circuits and the bilateral fin-line circuits, but also to the unilateral and insulated fin-line circuits (Fig. 1). Since the analysis portion of the algorithm is based on the residue-calculus technique [6] and a generalized scattering parameter method [7], it is mathematically exact and numerically very efficient, as the convergence is guaranteed. Filters thus designed have been fabricated and tested in *Ka*-band with good agreement with the design.

II. Theory

The CAD program consists of an optimization routine and an analysis routine. We describe the analysis routine first. The analysis is carried out in three steps. First, a limiting case of a single junction created by a semi-infinite septum in a waveguide is analyzed. This structure may be analyzed exactly using the residue-calculus technique [6] to obtain a closed-form expression for the scattering matrix. The second step is to calculate the scattering parameters for a finite-length septum. This is done by placing two junctions back to back, and utilizing the concept of the generalized scattering matrix [7], which takes into account the interaction between junctions by not only the propagating modes but also all the evanescent modes. Finally, to combine several septums into a filter circuit, the generalized *S*-matrix technique is applied again to obtain the total scattering parameters of the composite structure.

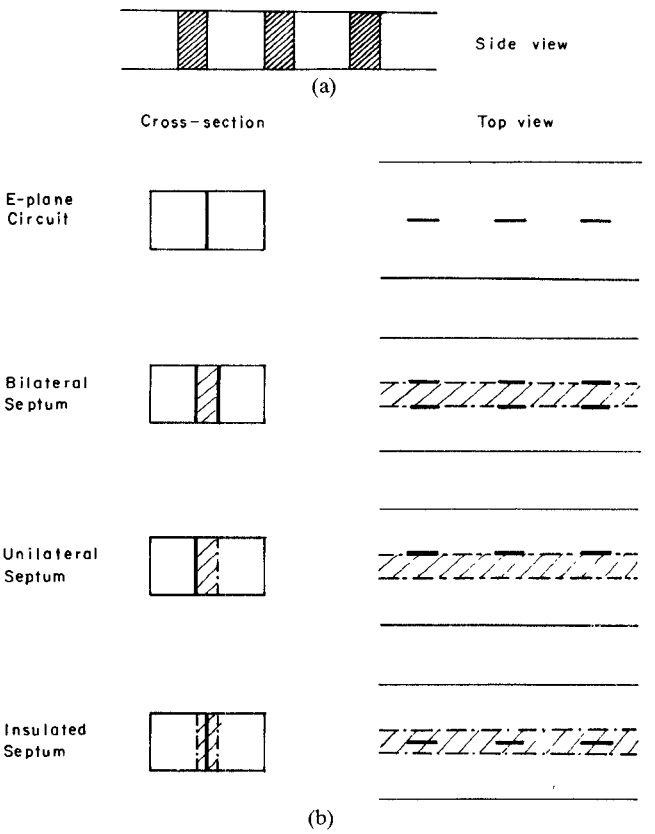

Fig. 1. Class of *E*-plane filter structures. (a) Side view. (b) Cross section and top view.

A. Semi-Infinite Septum

Let us consider an infinitesimally thin semi-infinite septum in a waveguide inhomogeneously filled with four

Manuscript received March 5, 1982; revised April 20, 1982. This work was supported in part by the U.S. Army Research Office Contract DAAG29-81-K-0053.

Y. C. Shih and T. Itoh are with the Department of Electrical Engineering, University of Texas, Austin, TX 78712.

L. Q. Bui is with the Hughes Aircraft Company, Electron Dynamics Division, Torrance, CA 90509.

0018-9480/83/0200-0135$01.00 ©1983 IEEE

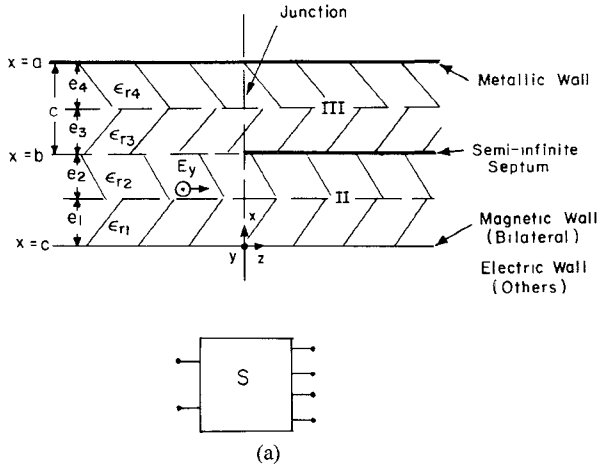

(a)

$$[S] = \begin{bmatrix} [S_{11}] & [S_{12}] & [S_{13}] \\ [S_{21}] & [S_{22}] & [S_{23}] \\ [S_{31}] & [S_{32}] & [S_{33}] \end{bmatrix}$$

(b)

Fig. 2. Characterization of the edge of septum. (a) Geometry. (b) Matrix representation.

dielectric slabs as shown in Fig. 2(a). This is a generalized structure for which values of the thickness and dielectric constant of each layer can be chosen to represent the structures in Fig. 1(b). (Note that for the case of bilateral fin-lines, a magnetic wall is introduced at the center of the waveguide and only the region above the magnetic wall is considered. Such a region represents the upper half of the bilateral fin-line due to the symmetry of the structure.) It is then subdivided into three regions at the junction $z = 0$, with each region consisting of a uniform waveguide which possesses known eigenmodes and corresponding propagation constants.

Assuming a TE_{10}-type incident wave, the excited fields are composed of the TE_{no}-type waves since there are no structural variations in the y-direction. Therefore, the existing modal fields consist of only E_y, H_x, and H_z components. The total fields in each region are then expanded in terms of the eigenmodes. After matching the tangential field components at $z = 0$, and making use of the orthogonality of the eigenmodes, an infinite set of equations results. Since the existence of the stratified dielectric layer does not affect the edge condition of the septum, the equations are of the same form as that for a bifurcated waveguide described in [6] and the scattering parameters of the junction are obtainable by the residue-calculus technique.

The resulting scattering matrix has nine elements, each of which is also a matrix of infinite dimension. The terms in each element are of the form of an infinite product multiplied by some constant coefficient. They are summarized in the following:

$$S_{11}(m,p) = -\frac{H_p}{H_m} e^{-L(\gamma'_m+\gamma'_p)} \frac{(\gamma''_m-\gamma'_m)(\gamma'''_m-\gamma'_m)}{(\gamma''_m+\gamma'_p)(\gamma'''_m+\gamma'_p)} \cdot f(m,-\gamma'_m,\gamma'_p) \quad (1a)$$

$$S_{21}(m,p) = \frac{H_p F_m}{2\gamma''_m} e^{L(\gamma''_m-\gamma'_p)} \frac{1}{(\gamma''_m-\gamma'_p)} \cdot f(0,\gamma''_m,\gamma'_p) \quad (1b)$$

$$S_{31}(m,p) = \frac{H_p G_m}{2\gamma'''_m} e^{L(\gamma'''_m-\gamma'_p)} \frac{1}{(\gamma'''_m-\gamma'_p)} \cdot f(0,\gamma'''_m,\gamma'_p) \quad (1c)$$

$$S_{12}(m,p) = -\frac{H_m F_p}{2\gamma'_m} e^{L(\gamma''_p-\gamma'_m)} \frac{1}{(\gamma'_m-\gamma''_p)} \cdot f(0,\gamma''_p,\gamma'_m) \quad (1d)$$

$$S_{22}(m,p) = -\frac{F_p}{F_m} e^{L(\gamma'_m+\gamma''_p)} \frac{(\gamma'''_m+\gamma''_p)(\gamma'_m-\gamma''_m)}{(\gamma'''_m-\gamma''_m)(\gamma'_m+\gamma''_p)} \cdot f(m,\gamma''_p,-\gamma''_m) \quad (1e)$$

$$S_{32}(m,p) = -\frac{F_p}{G_m} e^{L(\gamma'''_m+\gamma''_p)} \frac{(\gamma''_m+\gamma''_p)(\gamma'_m-\gamma'''_m)}{(\gamma''_m-\gamma'''_m)(\gamma'_m+\gamma''_p)} \cdot f(m,\gamma''_p,-\gamma'''_m) \quad (1f)$$

$$S_{13}(m,p) = -\frac{H_m G_p}{2\gamma'_m} e^{L(\gamma'''_p-\gamma'_m)} \frac{1}{(\gamma'_m-\gamma'''_p)} \cdot f(0,\gamma'''_p,\gamma'_m) \quad (1g)$$

$$S_{23}(m,p) = -\frac{G_p}{F_m} e^{L(\gamma''_m+\gamma'''_p)} \frac{(\gamma'''_m+\gamma'''_p)(\gamma'_m-\gamma''_m)}{(\gamma'''_m-\gamma''_m)(\gamma'_m+\gamma'''_p)} \cdot f(m,\gamma'''_p,-\gamma''_m) \quad (1h)$$

$$S_{33}(m,p) = -\frac{G_p}{G_m} e^{L(\gamma'''_m+\gamma'''_p)} \frac{(\gamma''_m+\gamma'''_p)(\gamma'_m-\gamma'''_m)}{(\gamma''_m-\gamma'''_m)(\gamma'_m-\gamma'''_p)} \cdot f(m,\gamma'''_p,-\gamma'''_m) \quad (1i)$$

where

$$L = \frac{b}{\pi}\ln\left(\frac{a}{b}\right) + \frac{c}{\pi}\ln\left(\frac{a}{c}\right)$$

$$f(m,\gamma_1,\gamma_2) = \prod_{\substack{n=1 \\ n\neq m}}^{\infty} \frac{(\gamma'_n+\gamma_2)(\gamma''_n+\gamma_1)(\gamma'''_n+\gamma_1)}{(\gamma'_n+\gamma_1)(\gamma''_n+\gamma_2)(\gamma'''_n+\gamma_2)}$$

where γ'_i, γ''_i, and γ'''_i are the propagation constants of the ith mode in Regions I, II, and III, respectively. F_i, G_i, and H_i are parameters determined readily for a given structure (see Appendix I). The notation $S_{ij}(m,p)$ stands for the scattering coefficient of the mth order mode.

B. Septum with Finite Length

With the knowledge of the scattering parameters for a single junction, the generalized scattering matrix technique is applied to obtain a two-port scattering matrix as

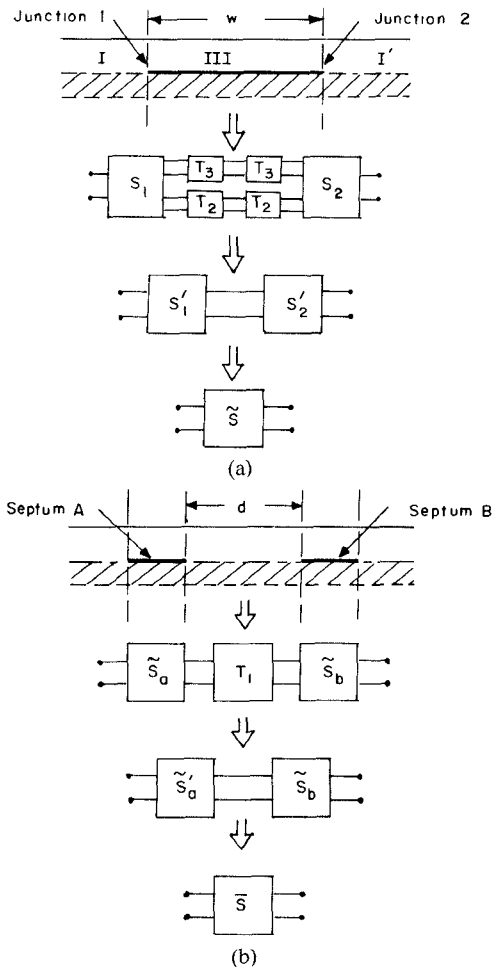

Fig. 3. *S*-parameter derivation. (a) For a single septum. (b) Cascaded septum.

shown in Fig. 3(a). Suppose now that the TE-type wave from Region I is incident upon Junction 1. At this junction, fields are reflected back into Region I, and transmitted into Regions II and III. After traveling a distance w, part of the wave transmitted into Regions II and III is reflected back and part is transmitted into Region I' at Junction 2. This process continues until the intensity of the reflected wave dies out. The multiple-reflection phenomenon between Junctions 1 and 2 is implied in a matrix manipulation which yields the scattering matrix for a finite length septum.

Referring to Fig. 3(a), S_1 and S_2 represent the scattering matrices for isolated Junctions 1 and 2 (i.e., for semi-infinite septums), respectively. From (1), we obtain the value of the elements in both matrices. Since the characteristics of these two junctions are essentially the same except for the opposite orientation, we have

$$S_2 = S_1^T. \tag{2}$$

We now define the transmission matrix

$$T = \begin{bmatrix} [I] & [0] & [0] \\ [0] & [T_2] & [0] \\ [0] & [0] & [T_3] \end{bmatrix} \tag{3}$$

where $[I]$ and $[0]$ are the identity matrix and the zero matrix, respectively, and the matrices $[T_2]$ and $[T_3]$ are of infinite size and represent the wave propagating (for propagation modes) or attenuating (for evanescent modes) for a distance of $w/2$ in guided Regions II and III, respectively. The combination of the transmission matrix along with S_1 and S_2 results in S_1' and S_2'

$$S_1' = TS_1T \tag{4}$$

$$S_2' = TS_2T = S_1^T. \tag{5}$$

A further combination of S_1' and S_2' then yields the composite scattering matrix $\tilde{S}$ for the septum of length w, viewed from I at $z = 0$ and from I' at $z = w$.

C. Filter Structures

For the final step of the analysis, several finite length septums are cascaded with appropriate separations to form a filter circuit. This is done by using the same techniques used in Section II-B described above. The procedure depicted in Fig. 3(b) shows the cascading of two septums represented by $\tilde{S}_a$ and $\tilde{S}_b$. The combination of $\tilde{S}_a$ and the transmission matrix T_1 results in matrix $\tilde{S}_a'$ which is further combined with $\tilde{S}_b$ to yield $\bar{S}$, the total scattering matrix of two septums with a separation of d. This procedure may be repeated to obtain the scattering parameters of a filter consisting of any number of septums.

III. Design

Based on the above analysis, a computer program is developed to calculate the total scattering parameters for a filter structure with given design parameters. Although the analysis is formally exact, in practice the infinite product in (1) and the infinite dimension of the elements in the scattering matrices need to be truncated. To obtain a very accurate result for (1), at least 300 terms should be retained. The calculation of the products here is efficient, since only readily known propagation constants are involved. Furthermore, this equation needs to be evaluated only once for a design assignment at each frequency point, since the scattering parameters of the semi-infinite septum depend only on the waveguide size and dielectric properties which are constant factors in a design.

For most applications, the fundamental mode is below cutoff in the narrow waveguide section and all of the higher order modes are evanescent in the wide waveguide. Therefore, only the first few accessible modes [8] are essentially responsible for the coupling between resonators. For most cases, only two or three modes are required to describe accurate scattering behavior. Notice that the number of modes considered here indicates the dimension of the matrices to be manipulated. The calculation includes a number of complex matrix multiplications and inversions. This analysis is efficient mainly due to the fact that only two or three modes are required.

Based on the analysis program, an optimization computer program applying the quasi-Newton method [9] is used which varies the input parameters until a desired

value of the insertion loss for a given bandwidth is obtained. To do this, an error function $F(\bar{x})$ to be minimized is defined

$$F(\bar{x}) = \sum_{N_s} \left(\frac{L_s}{|S_{21}|} \right)^2 + \sum_{N_p} \left(\frac{|S_{21}|}{L_s} \right)^2 \tag{6}$$

where N_s and N_p are the number of frequency sampling points in the stopband and passband, respectively, L_s and L_p are the minimum stopband and maximum passband attenuation levels, respectively, and $|S_{21}|$ is the calculated value of the filter attenuation. For a given thickness of the dielectric, the parameters $\bar{x}$ to be optimized are the septum lengths and resonator lengths.

To prevent the program from approaching nonrealizable or nonphysical results, upper and lower bounds of each parameter are specified

$$x_{li} < x_i < x_{ui}. \tag{7}$$

The constrained parameters are then reduced into essentially unconstrained ones by the transformation [10]

$$x_i = x_{li} + \frac{1}{\pi}(x_{ui} - x_{li}) \cot^{-1} x_i' \tag{8}$$

where $-\infty < x_i' < \infty$, but only solutions within the range

$$0 < \cot^{-1} x_i' < \pi \tag{9}$$

are allowed. This transformation has a penalizing effect upon the parameters in the vicinity of the upper and lower bounds.

For the optimization procedure, the first two modes in each subregion are considered; the final design values are calculated with three modes. The total computing time for optimizing a five-resonator filter was about 2 min on a CDC Dual Cyber 170/750.

IV. Results and Discussion

In an earlier publication [11], it has been pointed out that the Q-factor of insulated fin-lines is inferior to that of bilateral fin-lines. Therefore, in this study, bandpass filters have been designed using only bilateral and unilateral fin-line configurations. Some typical designs for *Ka*-band applications are shown in Figs. 4, 6, and 7 fabricated on RT/Duroid substrates. Notice that the resonators are very weakly coupled by wide septums. In such cases, the septum cannot be represented by simple shunt-inductance equivalent circuits. Instead, it has to be represented by an equivalent T network [1]. Since the equivalent circuits are useful in conventional circuit design and are helpful for good initial guesses in the optimization procedure, this topic is discussed briefly in Appendix II.

The five-resonator filter design in Fig. 4 is a bilateral fin-line in which the hatched portion indicates metal on both sides of the substrate. The center frequency is 38.85 GHz, the 0.1-dB ripple bandwidth is 1.1 GHz, and the skirt selectivity at 500 MHz away from either edge of the passband is -40 dB. Measured characteristics of this filter are shown in Fig. 5. Computed responses are also plotted for comparison. Shapes of the calculated and measured

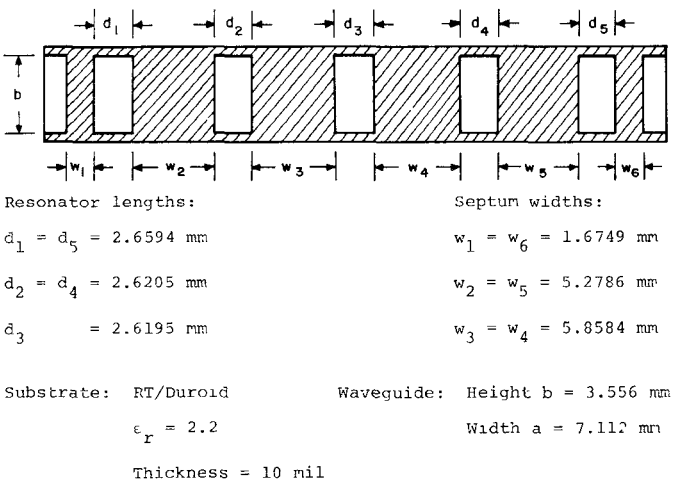

Fig. 4 Design example (five-resonator *Ka*-band bilateral fin-line filter)

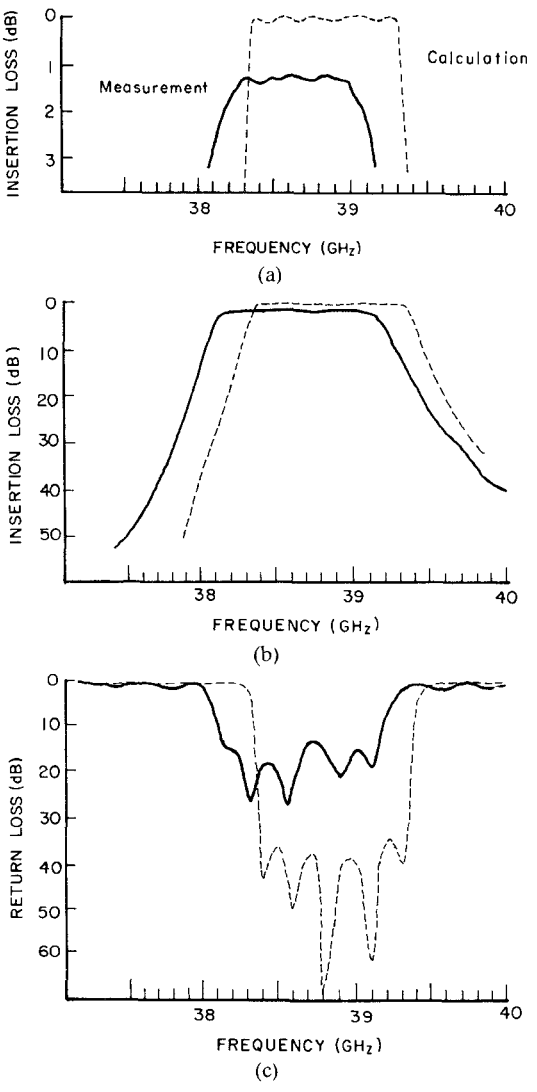

Fig. 5. Frequency responses for the filter in Fig. 4. (a) Expanded view of insertion loss. (b) Insertion loss characteristics. (c) Return loss characteristics.

response curves agree extremely well. Measured insertion loss in the passband is less than 1.3 dB of which 0.3 dB is associated with the test fixture. The measured center

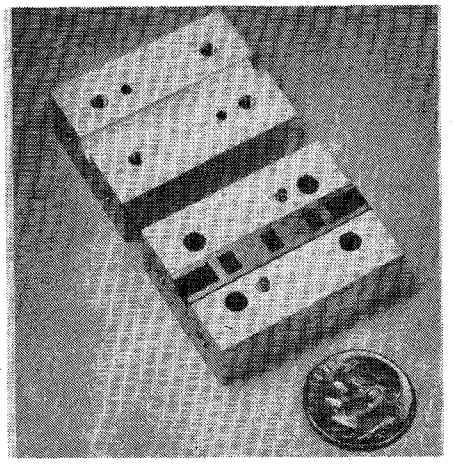

Fig. 6. Three-resonator *Ka*-band bilateral fin-line filter. Resonator length: $d_1 = d_3 = 2.6559$ mm; $d_2 = 2.6187$ mm. Septum width: $w_1 = w_4 = 1.7230$ mm; $w_2 = w_3 = 5.3628$ mm.

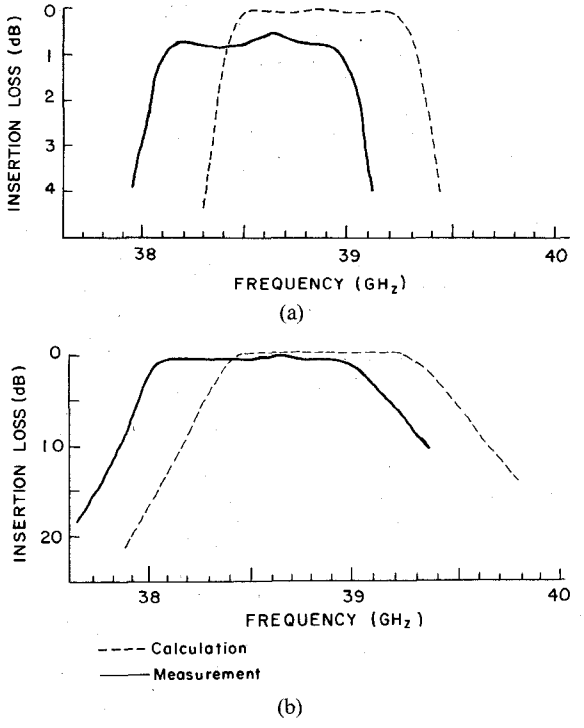

Fig. 7. Frequency responses for the filter in Fig. 6. (a) Expanded view of insertion loss. (b) Insertion loss characteristics. --- Calculation. —— Measurement.

frequency is shifted to the lower side by about 170 MHz which is less than 0.5 percent of the center frequency.

Fig. 6 shows a photograph of a three-resonator *Ka*-band bilateral fin-line filter printed on a 10-mil-thick RT/Duroid substrate. The design specifications for this filter were the same as those for the last one except for a decreased skirt selectivity of −20 dB. The measured results in Fig. 7 show that the insertion loss is less than 0.8 dB in the passband, including the fixture loss. The calculated and measured frequency responses again agree well; however, the measured center frequency is shifted down by about 300 MHz.

Bandpass filters have also been developed in unilateral fin-line configurations. A typical design for a three-resonator filter has the following specifications and dimensions:

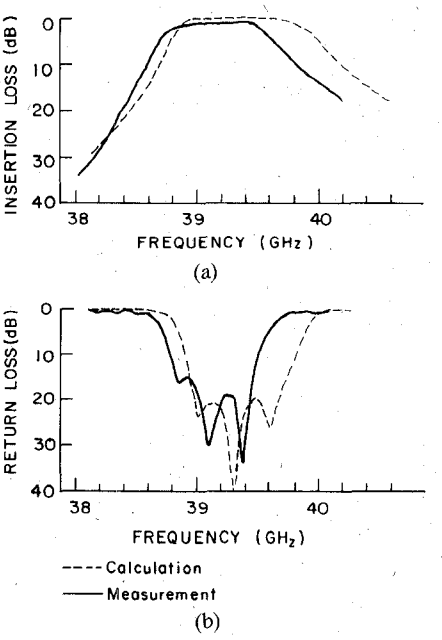

Fig. 8. Three-resonator *Ka*-band unilateral fin-line filter. --- Calculation. —— Measurement.

Resonator lengths	$d_1 = d_3 = 2.1568$ mm, $d_2 = 2.0879$ mm;
Septum widths	$w_1 = w_4 = 2.3325$ mm, $w_2 = w_3 = 6.8718$ mm;
Passband	39.0 ~ 39.7 GHz, Chebyshev response with 0.1-dB ripple; and
Skirt selectivity	−20 dB at 500 MHz away from passband edge.

The measured results in Fig. 8 show about 2-dB insertion loss in the passband and about 200-MHz downward shift for the center frequency.

In the experiments performed, the measured center frequencies are always lower than the calculated values. The deviations range from 170 MHz to 300 MHz. One cause of this shift is due to the way the filter is assembled. To support the substrate in the waveguide, 10-mil-deep grooves are machined into the top and bottom walls. An experimental study on this effect shows that within the quarter-wavelength range, the deeper the groove is made, the more the center frequency will shift down. In addition, another possible source of the discrepancy is the finite thickness of the metal fin. The thickness effect is minor at this frequency since the thickness of the copper cladding on the substrate is about 0.5 mil. However, it will become an important factor for higher frequency applications, such as *W*-band circuits. These effects are currently under study.

From the experiments, it has been observed that the insertion loss of a unilateral fin-line filter is always greater than that of a bilateral filter for similar design specifications. One possible explanation is that the dielectric loss of the unilateral filter is greater, while the conductor loss is about the same in both cases. In the case of bilateral fin-lines, little energy can penetrate into the very narrow space between the strips. Therefore, the energy is mainly

coupled through the wider empty waveguide section. In the unilateral case, the energy is coupled about evenly through the empty guide and the partially dielectric-filled guide region. Obviously, more dielectric loss is encountered in this case. By the same reasoning we can surmise that the conductor loss is about the same for both cases. Although the bilateral structure has copper cladding on both sides of the substrate, there is essentially no current flowing on the inner surface facing the dielectric. It is thus equivalent to a conducting strip with current flowing on the outer surface of both sides as in the unilateral case. Of course, these statements are strictly conjectural; further study is needed to verify them. This conjecture would also be applicable to the case of insulated fin-lines versus bilateral fin-lines.

Another point worth mentioning is the sensitivity of the filter structure to mechanical tolerances. Calculations show that for both cases, the center frequency shifts about 100 MHz if the fabrication error in resonator length is 1 mil. Also, if the dielectric substrate is shifted in the broadwall direction (x-direction) from its centered position, the filter's center frequency falls. This effect is much more noticeable with the unilateral structure. Therefore, the bilateral structure shows more promise from a constructional viewpoint.

V. Conclusions

We presented an efficient CAD algorithm based on an exact analysis for a class of E-plane bandpass filters. Filters for Ka-band applications have been fabricated based on the present design. Measured characteristics agree well with theoretical data. Extensive experiments show that the bilateral construction is more promising than the unilateral structure.

Appendix I
Expressions for H_n, F_n, and G_n

The coefficients H_n, F_n, and G_n are related to the structure geometry and the field distribution in Regions I, II, and III, respectively. They are derived from the overlapping integrals

$$\int_0^b \phi_m^{\mathrm{I}}(x)\phi_n^{\mathrm{II}}(x)\,dx = \frac{H_m F_n}{\gamma_n''^2 - \gamma_m'^2} \tag{A1}$$

$$\int_b^a \phi_m^{\mathrm{I}}(x)\phi_n^{\mathrm{III}}(x)\,dx = \frac{H_m G_n}{\gamma_n'''^2 - \gamma_m'^2} \tag{A2}$$

where $\phi_i^{\mathrm{I}}(x)$, $\phi_i^{\mathrm{II}}(x)$, and $\phi_i^{\mathrm{III}}(x)$ are the ith order orthonormal eigenfunctions for the E_y fields in Regions I, II, and III, respectively (refer to Fig. 2). The expressions for H_i, F_i, and G_i of different geometries are given in the following.

Metallic E-Plane Structure

$$H_n = \sqrt{\frac{2}{a}}\sin\frac{n\pi b}{a} \tag{A3a}$$

$$F_n = (-1)^n\sqrt{\frac{2}{b}}\,\frac{n\pi}{b} \tag{A3b}$$

$$G_n = (-1)^n\sqrt{\frac{2}{c}}\,\frac{n\pi}{c}. \tag{A3c}$$

Bilateral Fin-Line Structures

$$H_n = A_n\cos\xi_n b \tag{A4a}$$

$$F_n = (-1)^n\sqrt{\frac{2}{b}}\,\frac{\left(n-\frac{1}{2}\right)\pi}{b} \tag{A4b}$$

$$G_n = (-1)^n\sqrt{\frac{2}{c}}\,\frac{n\pi}{c} \tag{A4c}$$

where

$$A_n = \sqrt{2}\left[b + \frac{\sin\xi_n b\cos\xi_n b}{\xi_n} + \left(c - \frac{\sin\eta_n c\cos\eta_n c}{\eta_n}\right)\left(\frac{\cos\xi_n b}{\sin\eta_n c}\right)^2\right]^{-1/2}$$

and where ξ_n and η_n are x-components of nth order wavenumber in the dielectric and the air region, respectively.

Unilateral Fin-Line Structures

$$H_n = A_n C_n \sin\eta_n c \tag{A5a}$$

$$F_n = -B_n\xi_n'\frac{\sin\eta_n' e_1}{\sin\xi_n' e_2} \tag{A5b}$$

$$G_n = (-1)^n\sqrt{\frac{2}{c}}\cdot\frac{n\pi}{c} \tag{A5c}$$

where

$$A_n = \sqrt{2}\left[d - \frac{\sin\eta_n e_1\cos\eta_n e_1}{\eta_n} + \eta_n^2 e_2\left(\frac{\sin^2\eta_n e_1}{\eta_n^2} + \frac{\cos^2\eta_n e_1}{\xi_n^2}\right) + C_n^2\left(c - \frac{\sin\eta_n c\cos\eta_n c}{\eta_n}\right) + C_n\frac{\eta_n^2\sin\xi_n e_2}{\xi_n}\cdot\left(\frac{\sin\eta_n e_1\sin\eta_n c}{\eta_n^2} + \frac{\cos\eta_n e_1\cos\eta_n c}{\xi_n^2}\right)\right]^{-1/2}$$

$$C_n = \frac{\eta_n}{\sin\eta_n c}\left(\frac{\sin\eta_n e_1\cos\xi_n e_2}{\eta_n} + \frac{\sin\xi_n e_2\cos\eta_n e_1}{\xi_n}\right)$$

$$B_n = \sqrt{2}\left[e_1 - \frac{\sin\eta_n' e_1\cos\eta_n' e_1}{\eta_n'} + \left(e_2 - \frac{\sin\xi_n' e_2\cos\xi_n' e_2}{\xi_n'}\right)\left(\frac{\sin\eta_n' e_1}{\sin\xi_n' e_2}\right)^2\right]^{-1/2}$$

and where $\xi_n(\xi_n')$ and $\eta_n(\eta_n')$ are the nth order wavenumber of dielectric (air) part in Regions I and II, respectively.

Appendix II
Equivalent Circuit of a Strip

The equivalent T network for a finite-length septum is shown in Fig. 9. The values of the normalized reactance x_s and x_p are to be calculated from the scattering parameters

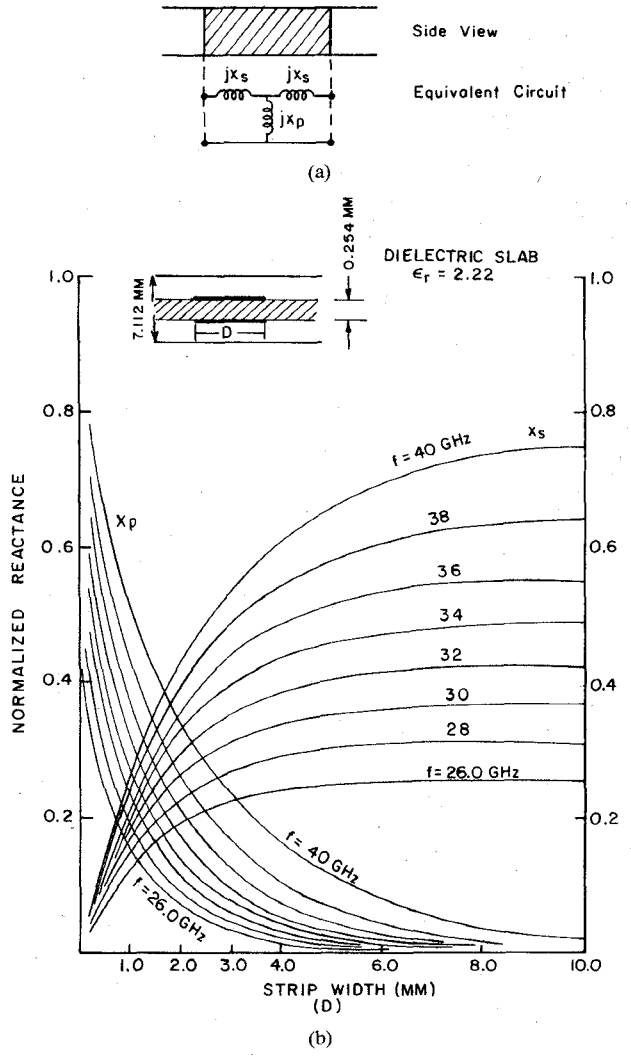

Fig. 9. Equivalent circuit for a finite-length septum. (a) Equivalent circuit. (b) Plot of reactances x_s and x_p versus septum length.

of a septum of length, say, w. Let the scattering matrix of the fundamental mode be

$$S = \begin{bmatrix} S_{11} & S_{12} \\ S_{21} & S_{22} \end{bmatrix}. \tag{A6}$$

For this reciprocal lossless two-port device, the following relations hold:

$$S_{12} = S_{21} \tag{A7}$$

$$S_{11} = S_{22} \tag{A8}$$

$$|S_{11}|^2 + |S_{22}|^2 = 1. \tag{A9}$$

These relations provide useful error-checking criteria for the numerical calculation.

If we convert the scattering matrix into impedance matrix and equate it to the impedance matrix of the equivalent T network, we have

$$[\bar{Z}] = [I+S][I-S]^{-1} = \begin{bmatrix} jx_s + jx_p & jx_p \\ jx_p & jx_s + jx_p \end{bmatrix} \tag{A10}$$

where I is the identity matrix. By equating the elements in the matrix on both sides, x_s and x_p are uniquely determined

$$jx_p = \frac{2S_{12}}{(1-S_{11})^2 - S_{12}^2} \tag{A11}$$

$$jx_s = \frac{1 - S_{12} + S_{11}}{1 - S_{11} + S_{12}}. \tag{A12}$$

Fig. 9 shows the calculated values for x_s and x_p as a function of septum length w with frequency as parameters.

References

[1] Y. Konishi and K. Uenakada, "The design of a bandpass filter with inductive strip-planar circuit mounted in waveguide," *IEEE Trans. Microwave Theory Tech.*, vol. MTT-22, pp. 869–873, Oct. 1974.

[2] Y. Tajima and Y. Sawayama, "Design and analysis of a waveguide-sandwich microwave filter," *IEEE Trans. Microwave Theory Tech.*, vol. MTT-22, pp. 839–841, Sept. 1974.

[3] P. J. Meier, "Integrated fin-line millimeter components," *IEEE Trans. Microwave Theory Tech.*, vol. MTT-22, pp. 1209–1216, Dec. 1974.

[4] A. M. K. Saad and K. Schünemann, "Design and performance of fin-line bandpass filters," *9th Eur. Microwave Conf.*, (Brighton, England), Sept. 17–20, 1979.

[5] F. Arndt *et al.*, "Low-insertion-loss fin-line filters for millimeter-wave applications," *11th Eur. Microwave Conf.* (Amsterdam, Netherlands), Sept. 7–10, 1981, pp. 309–314.

[6] R. Mittra and S. W. Lee, *Analytical Techniques in the Theory of Guided Waves*. New York: Macmillan, 1971, pp. 45–54.

[7] C. F. Vanblaricum, Jr. and R. Mittra, "A modified residue-calculus technique for solving a class of boundary value problems—Part II: Waveguide phased arrays, modulated surfaces, and diffraction gratings," *IEEE Trans. Microwave Theory Tech.*, vol. MTT-17, pp. 310–319, June 1969.

[8] T. E. Rozzi and W. F. G. Mecklenbräuker, "Wide-band network modeling of interacting inductive irises and steps," *IEEE Trans. Microwave Theory Tech.*, vol. MTT-23, pp. 235–245, Feb. 1975.

[9] Routin ZXMIN, IMSL Library 3 (for CDC Cyber 70/6000/7000 series). See IMSL Library Manual.

[10] J. W. Bandler, "Optimization method for computer-aided design," *IEEE Trans. Microwave Theory Tech.*, vol. MTT-17, pp. 533–562, Aug. 1969.

[11] P. J. Meier, "Equivalent relative permittivity and unloaded Q factor of integrated fin-line," *Electron. Lett.*, vol. 9, no. 7, pp. 162–163, Apr. 1973.

Yi-Chi Shih (SM'80) was born in Taiwan, the Republic of China, on February 8, 1955. He received the B. Eng. degree from National Taiwan University, Taiwan, R.O.C., in 1976, and the M.Sc. degree from the University of Ottawa, Ontario, Canada, in 1980, both in electrical engineering. Since 1980 he has been working toward the Ph.D. degree at The University of Texas at Austin.

His research interest includes the analysis and design of microwave and millimeter-wave components.

Tatsuo Itoh (SM'74–F'82) received the Ph.D. degree in electrical engineering from the University of Illinois, Urbana, in 1969. From September 1966 to April 1976 he was with the Electrical Engineering Department, University of Illinois. From April 1976 to August 1977 he was a Senior Research Engineer in the Radio Physics Laboratory, SRI International, Menlo Park, CA. From August 1977 to June 1978 he was an Associate Professor at the University of Kentucky, Lexington. In July 1978, he

joined the faculty at the University of Texas at Austin, where he is now a Professor of Electrical Engineering and Director of the Microwave Laboratory. During the summer 1979 he was a Guest Researcher at AEG-Telefunken, Ulm, West Germany.

Dr. Itoh is a member of the Institute of Electronics and Communication Engineers of Japan, Sigma Si, and Commission B of USNC/URSI. He serves on the Administrative Committee of IEEE Microwave Theory and Techniques Society. He is a Professional Engineer registered in the State of Texas.

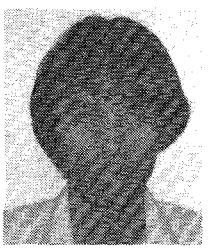

Long Q. Bui was born in Hue, South Vietnam, on May 6, 1952. He received the B.S. Degree in electrical engineering in 1976, and the M.S.E.E. degree in 1981, both from the University of Texas at Austin, TX.

He has been with Hughes Aircraft Company, Torrance, CA, since 1979 as a Member of Technical Staff on Advanced Component Developments for millimeter-wave applications. His main research interests are concerned with planar circuit techniques for mixers, filters, multiplier designs, and computeraided techniques for design and manufacture.

Integrated Fin-Line Components and Subsystems at 60 and 94 GHZ

WOLFGANG MENZEL AND HEINRICH CALLSEN

Abstract—**This paper describes fin-line receiver components for the frequency ranges around 60 and 94 GHz. In detail, the design and performance of balanced mixers, p-i-n-diode attenuators, and p-i-n-diode double throw switches will be presented. Next, the integration of such components (partly together with fin-line Gunn oscillators) will be demonstrated, showing a number of advantages concerning size, weight, losses, cost, and ruggedness.**

I. Introduction

THE APPLICATION of millimeter-wave frequencies for radar, radiometry, and communication has found an increasing importance during the last years. The demand for reliable low-cost millimeter-wave components and subsystems has led to the development of planar integrated millimeter-wave circuits. One possible choice, the fin-line technique, is employed in the circuits reported in this paper.

Fin-line circuits exhibit a number of advantages such as broad bandwidth, easy implementation of semiconductors, flexible design, simple, reproducible, and cost effective production, and the possibility of integrating several components on the same substrate. On the other hand, higher losses compared with standard metal waveguides restrict the application of fin-line for high-Q filters and for high-power circuits. The latter, however, is presently of minor importance.

A great number of fin-line papers have been published, e.g., [1]–[13], dealing with the calculation of fin-line parameters and discontinuities, fin-line components, and the integration of several components into subsystems. A detailed overview and an extensive reference list concerning fin-line technique is given in [14].

This paper presents design and performance of integrated receiver front-ends at 60 and 94 GHz. In the next two sections, the individual components of these front-ends, such as mixers, p-i-n-diode attenuators, and SPDT switches will be described. Following this, the integration of these components on a single substrate will be shown, yielding a number of advantages over standard waveguide components as well as over discrete-component fin-line circuits.

II. Fin-Line p-i-n-Diode Attenuators and Switches

Fin-line p-i-n-diode devices have been built to provide electronically tunable attenuators, switches, and modulators up to 100 GHz and beyond [7]. Fig. 1 shows the basic

Manuscript received April 30, 1982; revised July 20, 1982.

The authors are with AEG–Telefunken, A1 E32, D-7900 Ulm, West Germany.

0018-9480/83/0200-0142$01.00 ©1983 IEEE